Brownian parametric quantum oscillator with dissipation

Christine Zerbe and Peter Hänggi
Institute of Physics, University of Augsburg, Memmingerstrasse 6, D-86135 Augsburg, Germany
(Received 4 April 1995)

We study the quantum fluctuational properties of a parametric oscillator with and without coupling to an Ohmic environment. After considering the momentum and coordinate variances as a function of initial squeezing for the undamped dynamics, we invoke the functional integral method to derive the fully exact reduced density matrix for parametric dissipative quantum Brownian motion, covering the whole temperature regime from $T = 0$ up to the classical limit at room temperatures. Moreover, we present the exact result for the quantum master equation for both the density matrix and the corresponding Wigner function. The time evolution of the covariance matrix elements of damped quantum fluctuations is studied numerically. These variances undergo within the regime of global stability asymptotic, periodic oscillations. As an interesting result, we find that the minima of these oscillations fall below the corresponding thermal equilibrium values.

PACS number(s): 05.30.−d, 05.40.+j, 32.80.Pj

I. INTRODUCTION

The study of the quantum dynamics of a particle moving in a time-dependent potential has prompted a flurry of literature over the past few years [1]. Due to the nonlinear forces inherent in most models they can be solved by numerical means only or within certain approximations. In this paper we shall discuss one of the few exactly solvable time-dependent quantum systems, both with and without coupling to an Ohmic environment. A short account of our work appeared in Ref. [2].

The system under study is a parametric one-dimensional oscillator for the coordinate x (with mass m and angular frequency ω_0) described by the time-dependent potential

$$V(x,t) = \frac{1}{2}m[\omega_0^2 + \epsilon\cos(\Omega t + \varphi)]x^2. \quad (1)$$

The parametric modulation is characterized by the amplitude ϵ, the modulation frequency Ω, and an initial phase φ. We assume that the phase is not known, i.e., it is equally distributed between 0 and 2π. For $\epsilon = 0$ the potential (1) becomes the potential of a harmonic oscillator — or of a parabolic barrier, because we also allow negative values for ω_0^2.

This potential has several possible physical applications. One major application is the study of the quadrupole ion trap, also termed *Paul trap*, in the quantum regime [3,4]. Another suggested application is the generation of squeezed states [5,6].

A major objective is the study of the influence of dissipation on the quantum mechanics of the parametric oscillator in (1). In doing so, we shall couple the time-dependent quantum system in (1) to a bath composed of infinite many oscillators. This system-plus-reservoir approach for the description of quantum dissipation has been pioneered during the sixties [7] for purely harmonic systems. For nonlinear system dynamics coupled to a bath of harmonic oscillators [8] this system-plus-harmonic bath presents the state of the art in the description of quantum dissipation [9]. Therefore, although we deal with quadratic interactions only, the results are — due to the inherent time dependence of the potential and the huge number of bath degrees of freedom — nontrivial.

We start within classical mechanics in Sec. II and give a brief review of the classical parametric oscillator. A survey of the quantum parametric oscillator without dissipation is presented in Sec. III. Additionally, we present a barely known method to construct the propagator for this system. Based upon these results we study the problem of *parametric dissipative quantum Brownian motion* in the time-dependent potential (Sec. IV). We introduce the coupling to an Ohmic heat bath and use the Feynman-Vernon real time influence functional formalism [10,11] to derive the exact evolution operator for the reduced density matrix. We also present the master equation for this system. On the basis of these exact results we calculate and discuss time-dependent mean values and variances. We conclude with a brief summary in Sec. V.

II. THE CLASSICAL PARAMETRIC OSCILLATOR

In a linear quantum mechanical system — damped or undamped — the average motion is governed by Ehrenfest's theorem, which coincides with the corresponding classical problem. Therefore, we first recall some results for the classical parametric oscillator. The equation of motion for a damped particle in the potential (1) reads

$$m\ddot{x} + m\gamma\dot{x} + m\omega^2(t,\varphi)x = 0$$

$$\text{with } \omega^2(t,\varphi) = \omega_0^2 + \epsilon\cos(\Omega t + \varphi). \quad (2)$$

The parameter γ characterizes Ohmic damping. The introduction of the scaled parameters $\bar{t} = \Omega t/2$, $\bar{\omega}_0^2 =$

$4\omega_0^2/\Omega^2$, $\bar{\epsilon} = 2\epsilon/\Omega^2$, and $\bar{\gamma} = 2\gamma/\Omega$ renders the normalized damped equation of motion for a parametric oscillator, i.e.,

$$\ddot{x} + \bar{\gamma}\dot{x} + \bar{\omega}^2(\bar{t}, \varphi)x = 0, \tag{3}$$

where $\bar{\omega}^2(\bar{t}, \varphi) = \bar{\omega}_0^2 + 2\bar{\epsilon}\cos(2\bar{t} + \varphi)$. In this section we shall exclusively use the normalized form (3) and hence drop the overbars for the sake of convenience. With the substitution $x = y\exp(-\gamma t/2)$ one can remove the damping contribution such that Eq. (3) can be cast into the standard form of a (formally undamped) Mathieu equation [12], with a friction-renormalized angular frequency

$$\ddot{y} + \left[\omega_0^2 - \frac{\gamma^2}{4} + 2\epsilon\cos(2t + \varphi)\right] y = 0. \tag{4}$$

In general this equation cannot be solved in explicit form. From the Floquet theory for an ordinary second-order differential equation with periodic coefficients we know that there exist two independent solutions of (4) of the form [12]

$$\begin{aligned} g_1(t;\varphi) &= e^{i\nu(t+\varphi/2)}p(t + \varphi/2), \\ g_2(t;\varphi) &= g_1(-t;-\varphi), \end{aligned} \tag{5}$$

with $p(t)$ a periodic function of time, i.e., $p(t + \pi) = p(t)$. The constant ν is called the *characteristic* or *Floquet exponent*. For $\epsilon = 0$ the Floquet exponent ν and the periodic function $p(t)$ become

$$\nu = \sqrt{\omega_0^2 - \frac{\gamma^2}{4}}, \quad p(t) = 1 \qquad \text{if } \omega_0^2 > \frac{\gamma^2}{4}$$

or

$$\nu = i\sqrt{\frac{\gamma^2}{4} - \omega_0^2}, \quad p(t) = 1 \qquad \text{if } \omega_0^2 < \frac{\gamma^2}{4}. \tag{6}$$

Hence the familiar results for the damped harmonic oscillator are recovered.

We see that the Floquet exponent ν governs the global behavior of the solution. In regions of parameter space where ν is real, but not an integer, both fundamental solutions are bounded for all times. The general solution to (4), which is a linear combination of g_1 and g_2, is then called stable. If ν becomes complex, one of the solutions grows exponentially as $t \to \infty$. The general solution is termed unstable. In the special case when ν is a whole number, which occurs on the "boundary" between stability and instability, it can be shown that the solutions g_1 and g_2 are not linearly independent. One of the solutions is a periodic function with period π or 2π; the second independent solution is found to be unstable. The diagram in Fig. 1(a) depicts the stable [white areas in Fig. 1(a)] and unstable regions (shaded areas) of the Mathieu equation (4). Changing the sign of ϵ, i.e., $\epsilon \to -\epsilon$, is equivalent to a phase shift $\varphi \to \varphi' = \varphi + \pi$. This phase, however, has no influence on the stability of the solutions. The diagram is therefore symmetric to the $(\omega_0^2 - \gamma^2/4)$ axis.

After transforming back from $y(t) \to x(t)$, a general solution of Eq. (3) may be expressed in the form

$$\begin{aligned} x(t) = {} & c_1 e^{(i\nu-\gamma/2)t+i\nu\varphi/2}p(t + \varphi/2) \\ & + c_2 e^{-(i\nu+\gamma/2)t-i\nu\varphi/2}p(-t - \varphi/2). \end{aligned} \tag{7}$$

The constants c_1, c_2 are determined through the initial values of $x(t)$ and $\dot{x}(t)$. We can — dependent on the parameter values — distinguish between three different kinds of asymptotic ($t \to \infty$) solutions. If ν is real or complex with $\mathrm{Im}(\nu) < \gamma/2$, then $x(t) \to 0$. The solution $x(t)$ is purely oscillating with period π or 2π, if $\mathrm{Im}(\nu) = \gamma/2$. If $\mathrm{Im}(\nu) > \gamma/2$ the solution $x(t)$ grows exponentially. Figure 1(b) shows the stability diagram for $\gamma = 0$ and $\gamma = 0.4$. The solid lines form the stability diagram for zero friction, while the dotted lines give the new stability zones at finite friction $\gamma = 0.4$. The unstable regions are reduced to the shaded areas. The effect of damping increases the regions of bounded solutions;

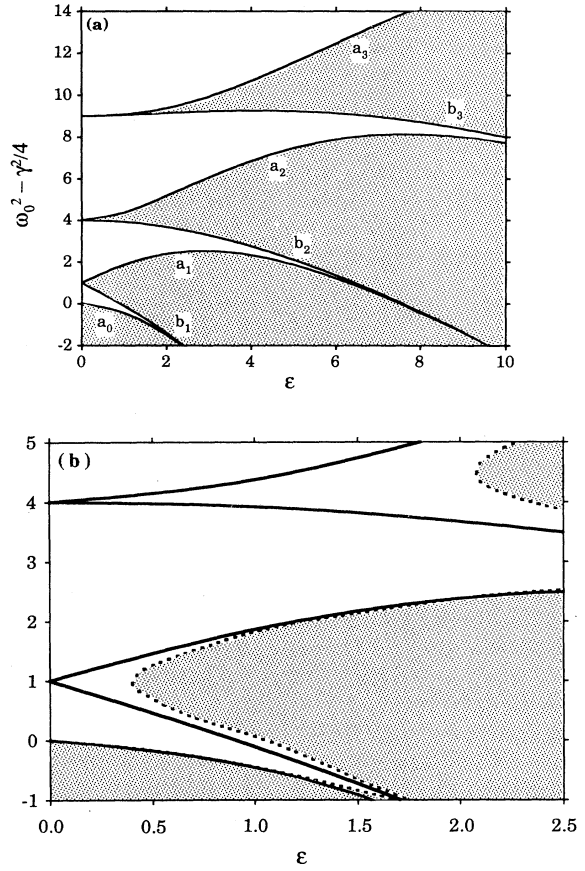

FIG. 1. (a) Stability chart for the Mathieu equation (4) with shifted angular frequency $\omega_0^2 \to \omega_0^2 - \gamma^2/4$. The shaded areas, being bounded by the lines a_n and b_{n+1}, $n = 0, 1, 2, \ldots$, denote the regions of unstable solutions. The diagram is symmetrical about the ordinate axis. (b) Stability diagram for the damped parametric oscillator Eq. (3) for the values $\gamma = 0$ and $\gamma = 0.4$. The solid lines denote the boundaries for stability for $\gamma = 0$. With finite friction, i.e., $\gamma = 0.4$, the regions of bounded solutions become extended as characterized by the dotted lines. The shaded areas denote the corresponding regions of instability.

in particular, the zones of unbounded solutions no longer reach the ω_0^2 axis.

For later simplification we introduce solutions to Eq. (4), ϕ_1 and ϕ_2, with the special initial values at time $t_0 = 0$

$$\phi_1(t_0;\varphi) = 0, \qquad \phi_2(t_0;\varphi) = 1,$$
$$\dot{\phi}_1(t_0;\varphi) = 1, \qquad \dot{\phi}_2(t_0;\varphi) = 0. \tag{8}$$

Because the Wronskian for the Mathieu equation is independent of the time [12], ϕ_1 and ϕ_2 fulfill the relation

$$\dot{\phi}_1(t;\varphi)\phi_2(t;\varphi) - \phi_1(t;\varphi)\dot{\phi}_2(t;\varphi) = 1. \tag{9}$$

Whenever we need explicit values for ϕ_1 and ϕ_2 we calculate them via a numerical integration of the differential equation in (4).

The combination G of solutions ϕ_1 and ϕ_2

$$G(t,s;\varphi) = \phi_1(t;\varphi)\phi_2(s;\varphi) - \phi_1(s;\varphi)\phi_2(t;\varphi) \tag{10}$$

will also proof useful in the following. By insertion of ϕ_1 and ϕ_2 into (10) it is easy to show the relations

$$G(t,s;\varphi) = -G(t,t';\varphi)\frac{\partial G(s,t';\varphi)}{\partial t'} + G(s,t';\varphi)\frac{\partial G(t,t';\varphi)}{\partial t'} \tag{11}$$

and

$$G(t,s;\varphi) = -G(s,t;\varphi). \tag{12}$$

III. THE QUANTUM PARAMETRIC OSCILLATOR

Introduction of the scaled quantities $\bar{x} = \sqrt{m\Omega/2\hbar}x$ and $\bar{t} = \Omega t/2$ yields the dimensionless Schrödinger equation for the potential (1), i.e.,

$$i\dot{\Psi}(\bar{x},\bar{t}) = \left[-\frac{1}{2}\partial_{\bar{x}}^2 + \frac{1}{2}\bar{\omega}^2(\bar{t})\bar{x}^2\right]\Psi, \tag{13}$$

with $\bar{\omega}^2(\bar{t}) = \bar{\omega}_0^2 + 2\bar{\epsilon}\cos(2\bar{t})$, $\bar{\omega}_0^2 = 4\omega_0^2/\Omega^2$, and $\bar{\epsilon} = 2\epsilon/\Omega^2$. Apart from $\bar{x}$, this is the same scale as in Sec. II. Again, we stick in this section to the scaled variables and henceforth omit the overbars for ease of notation. We have chosen the initial phase $\varphi = 0$, because, in contrast to Sec. IV, it provides no additional insight.

The periodicity of the Hamiltonian leads to Floquet form solutions of the Schrödinger equation [13]. With the initial time set $t_0 = 0$, a solution $\Psi_n(x,t)$ of Eq. (13) can be factorized as

$$\Psi_n(x,t) = \exp(-i\epsilon_n t)\chi_n(x,t),$$
$$\chi_n(x,t) = \chi_n(x,t+\pi). \tag{14}$$

The function χ_n is called a Floquet function and ϵ_n is the Floquet or quasienergy. Contrary to eigenfunctions of the time-independent problem, these Floquet functions are time-dependent and orthogonal only for fixed, equal time arguments, i.e., $\langle\chi_n(x,t)|\chi_m(x,t)\rangle = \delta_{nm}$. Because of the linearity of the system, χ_n and ϵ_n are fully determined through the solutions of the corresponding classical problem, i.e., solutions of Eq. (4) for vanishing constant γ

$$\ddot{x} + \omega^2(t)x = 0. \tag{15}$$

There are different approaches to the quantum mechanical problem; see, e.g., [3,4,14]. The wave functions and the Floquet energies for the whole parameter space were given first by Perelomov and Popov in Ref. [14]: In the stable region a *discrete spectrum* of quasienergies exists, which is given through $\epsilon_n = (n+\frac{1}{2})\nu$, $n = 0,1,2,...$, where ν is the Floquet exponent of the deterministic Mathieu equation (15). In the unstable regions and at the boundaries between these regions the spectrum becomes *continuous*: In the unstable region it is *doubly degenerate* and reads $\epsilon_k = k\ \mathrm{Im}(\nu)$, with k being a real number and running from $-\infty$ to ∞. The continuum is no longer degenerate at the boundaries where it is of the same form, with k ranging from 0 to ∞ only.

A. Propagator

The propagator for this system, obtained originally by Husimi [15], can be derived in a variety of ways, e.g., with Feynman's path integral method or by a canonical transformation into a harmonic oscillator as in [16]. In terms of the Floquet functions and the quasienergies, it is also possible to construct the propagator $K(x_f,t_f;x_i,t_i)$ directly in terms of a *spectral representation.* In this way we obtain

$$K(x_f,t_f;x_i,t_i) = \sum_{n=0}^{\infty}\chi_n(x_f,t_f)\chi_n^*(x_i,t_i) \times \exp\left[-\frac{i}{\hbar}\epsilon_n(t_f-t_i)\right]. \tag{16}$$

For a continuous spectrum the sum becomes an integral and we have to take into consideration possible degeneracies of the quasienergy spectrum. Doing so, we obtain for the propagator the explicit result

$$K(x_f,t_f;x_i,t_i) = \sqrt{\frac{1}{2\pi i G(t_f,t_i)}}\exp\left[\frac{i}{2G(t_f,t_i)}\left(x_f^2\frac{\partial G(t_f,t_i)}{\partial t_f} - 2x_ix_f - x_i^2\frac{\partial G(t_f,t_i)}{\partial t_i}\right)\right]$$
$$= e^{-i\pi m(t_f,t_i)/2}\sqrt{\frac{1}{2\pi i|G(t_f,t_i)|}}\exp\left[\frac{i}{2G(t_f,t_i)}\left(x_f^2\frac{\partial G(t_f,t_i)}{\partial t_f} - 2x_ix_f - x_i^2\frac{\partial G(t_f,t_i)}{\partial t_i}\right)\right]. \tag{17}$$

The function $G(t_f,t_i)$ is defined as in (10) with φ and γ set to zero. The Maslov correction $m(t,t_i)$ gives the number of zeros of $G(t,t_i)$ in the interval $[t_i,t]$, $m(t_i,t_i)=0$, and we used the definition of the root

$$G^{1/2}(t,t_i)=|G(t,t_i)|^{1/2}e^{i\pi m(t,t_i)/2}.$$

But this propagator (17) is valid only for times $t_f \neq t_m$. With t_m we denote the time when the mth zero of $G(t_f,t_i)$ occurs. To calculate the propagator at these so-called *caustics* we use the propagator property, namely,

$$K(x_n,t_n;x_i,t_i)$$

$$=\int_{-\infty}^{\infty}dx_c\,K(x_n,t_n;x_c,t_c)K(x_c,t_c;x_i,t_i). \quad (18)$$

This relation holds for any time order of t_i,t_c, and t_n. It is not necessary that $t_c<t_n$. We choose the intermediate time t_c so that $K(x_n,t_n;x_c,t_c)$ and $K(x_c,t_c;x_i,t_i)$ do not possess caustics at this point. With the relations (11) and (12) we find for the propagator at a caustic the explicit result

$$K(x_m,t_m;x_i,t_i)$$

$$=e^{-i\pi m(t_m,t_i)/2}\sqrt{|\partial G(t_m,t_i)/\partial t_i|}\times\delta\left[x_m-\frac{\partial G(t_i,t_m)}{\partial t_i}x_i\right]\times\exp\left\{\frac{i}{2}\left[\frac{\partial^2 G(t_m,t_i)}{\partial t_m\partial t_i}\Big/\frac{\partial G(t_m,t_i)}{\partial t_i}\right]x_m^2\right\}, \quad (19)$$

with $\partial G(t_m,t_i)/\partial t_i=[\partial G(t,t_i)/\partial t_i]_{|t=t_m}$.

B. Variances and squeezing

It has been demonstrated previously [5,6] by various methods that a time-dependent harmonic oscillator generates squeezed states. To study its squeezing properties in greater detail we compute the variances of the operators x and p with the Heisenberg equation of motion. For this linear system the mean value of the operator x follows the solution of the classical equation (15) and the mean value of the momentum is given as $\langle p\rangle=d\langle x\rangle/dt$.

The variances $\sigma_{xx}(t)\equiv\langle x^2\rangle-\langle x\rangle^2$, $\sigma_{xp}(t)\equiv\frac{1}{2}\langle xp+px\rangle-\langle x\rangle\langle p\rangle$, and $\sigma_{pp}(t)\equiv\langle p^2\rangle-\langle p\rangle^2$ satisfy the coupled set of equations

$$\dot\sigma_{xx}=2\sigma_{xp},\qquad \dot\sigma_{xp}=\sigma_{pp}-\omega^2(t)\sigma_{xx},\qquad \dot\sigma_{pp}=-2\omega^2(t)\sigma_{xp}. \quad (20)$$

By eliminating $\sigma_{xp}(t)$ and $\sigma_{pp}(t)$ from Eqs. (20) we find an equivalent third-order equation for $\sigma_{xx}(t)$

$$\dddot\sigma_{xx}+4\omega^2(t)\dot\sigma_{xx}+2\left\{\frac{d}{dt}[\omega^2(t)]\right\}\sigma_{xx}=0. \quad (21)$$

This equation is solved for a state that is prepared at time $t_0=0$ with the initial variances σ^0_{xx}, σ^0_{xp}, and σ^0_{pp}. The solution for the variance of the coordinate x then reads

$$\sigma_{xx}(t)=\sigma^0_{pp}\phi_1^2(t)+\sigma^0_{xx}\phi_2^2(t)+2\sigma^0_{xp}\phi_1(t)\phi_2(t), \quad (22)$$

where ϕ_1 and ϕ_2 are defined as before in (8). With (20) we find for the remaining variances the result

$$\sigma_{xp}(t)=\sigma^0_{pp}\phi_1(t)\dot\phi_1(t)+\sigma^0_{xx}\phi_2(t)\dot\phi_2(t)+\sigma^0_{xp}[\phi_1(t)\dot\phi_2(t)+\dot\phi_1(t)\phi_2(t)] \quad (23)$$

and

$$\sigma_{pp}(t)=\sigma^0_{pp}\dot\phi_1^2(t)+\sigma^0_{xx}\dot\phi_2^2(t)+2\sigma^0_{xp}\dot\phi_1(t)\dot\phi_2(t). \quad (24)$$

In contrast to the harmonic oscillator, the variances are always time-dependent quantities. They are bounded or increasing with time, like the solutions of the Mathieu equation in the corresponding region. To obtain explicit results we start at $t_0=0$ with a wave packet with minimum uncertainty $\sigma^0_{xx}=1/2r\sqrt{\omega_0^2+2\epsilon}$, $\sigma^0_{xp}=0$, and $\sigma^0_{pp}=r\sqrt{\omega_0^2+2\epsilon}/2$. This corresponds to a coherent, or squeezed, state of a harmonic oscillator with angular frequency $\omega_{\rm HO}=\sqrt{\omega_0^2+2\epsilon}=\omega(t_0=0)$. The parameter r characterizes the amount of squeezing of the initial state; $r=1$ refers to an unsqueezed initial state. With (22)–(24) it can be shown that the state does not remain a state of minimum uncertainty for all times, i.e.,

$$\sigma_{xx}(t)\sigma_{pp}(t)=\sigma^0_{xx}\sigma^0_{pp}+\sigma^2_{xp}(t). \quad (25)$$

Only for times when $\sigma_{xp}(t)$ equals zero is the initial uncertainty reattained. At these times $\sigma_{xx}(t)$ and $\sigma_{pp}(t)$ take on minimal or maximal values, as can be deduced from (20), i.e., maximal squeezing in one of the variances occurs. In Fig. 2 we plot the time variation of $\sigma_{xx}(t)$ for a fixed value of ω_0^2. Depending on the chosen parameters and the initial squeezing the results vary strongly. Figure 2(a) shows $\sigma_{xx}(t)$ for a squeezed state and different amplitudes of the parametric modulation ϵ. In Fig. 2(a) we can observe that *strong squeezing* — alternately in $\sigma_{xx}(t)$ and $\sigma_{pp}(t)$ — appears at certain times. For parameter values in the region of stability the amplitudes of the oscillations of the variances are small. Approaching the boundary of stability, the amplitudes become larger, and in the instable regime they grow to infinity as $t\to\infty$. It can be seen that the variation of ϵ changes the form and also the amplitude of the oscillations. In Fig. 2(b) variances are plotted for different squeezing parameters r.

IV. THE DISSIPATIVE QUANTUM BROWNIAN PARAMETRIC OSCILLATOR

To describe the influence of friction we couple our system bilinearly to an environment [7–11]. This environment is modeled by a linear system consisting of a set of noninteracting harmonic oscillators. The Hamiltonian of the coupled system assumes then the form

$$H(t) = H_{\rm osc}(t) + H_I + H_B, \tag{26}$$

where

$$H_{\rm osc}(t) = \frac{p^2}{2m} + \frac{1}{2}m[\omega_0^2 + \epsilon\cos(\Omega t + \varphi)]x^2,$$

is the Hamiltonian of the parametric quantum oscillator,

$$H_B = \sum_{\alpha=1}^{N}\frac{p_\alpha^2}{2m_\alpha} + \frac{1}{2}\sum_{\alpha=1}^{N} m_\alpha\omega_\alpha^2\xi_\alpha^2$$

is the Hamiltonian of the reservoir consisting of N oscillators with masses m_α, angular frequencies ω_α, momenta p_α, and coordinates ξ_α, and

$$H_I = -x\sum_{\alpha=1}^{N} c_\alpha\xi_\alpha + x^2\sum_{\alpha=1}^{N}\frac{c_\alpha^2}{2m_\alpha\omega_\alpha^2}$$

is the interaction Hamiltonian. The first term in H_I couples via the coupling strengths $\{c_\alpha\}$ the parametric oscillator to the bath. The interaction with the bath oscillators leads to a frequency shift in the parametric oscillator. This purely classical effect is removed with the second contribution in $H_{\rm I}$, termed the counterterm [17].

To obtain explicit results we need to specify the environment: We consider the bath and the parametric oscillator to be uncoupled initially. The heat bath is then in equilibrium at temperature T. At time $t_0 = 0$ the parametric oscillator and the heat bath are brought together. The total density matrix at $\{x_i, y_i, t_0\}$ can therefore be written as $\rho_{{\rm osc}+B}(x_i, y_i, t_0) = \rho_{\rm osc}(x_i, y_i, t_0)\rho_B(x_i, y_i, t_0)$, where $\rho_{\rm osc}(x_i, y_i, t_0)$ and $\rho_B(x_i, y_i, t_0)$ are the density operators of the parametric oscillator and the reservoir, respectively. Additionally, the bath consists of an infinite number of oscillators with densely distributed frequencies. Therefore we introduce a spectral density of the environment $I(\omega)$

$$I(\omega) = \pi\sum_{\alpha=1}^{N}\frac{c_\alpha^2}{2m_\alpha\omega_\alpha}\delta(\omega - \omega_\alpha). \tag{27}$$

Throughout this work we consider an Ohmic heat bath that is characterized through the spectral density $I(\omega) = m\gamma\omega$.

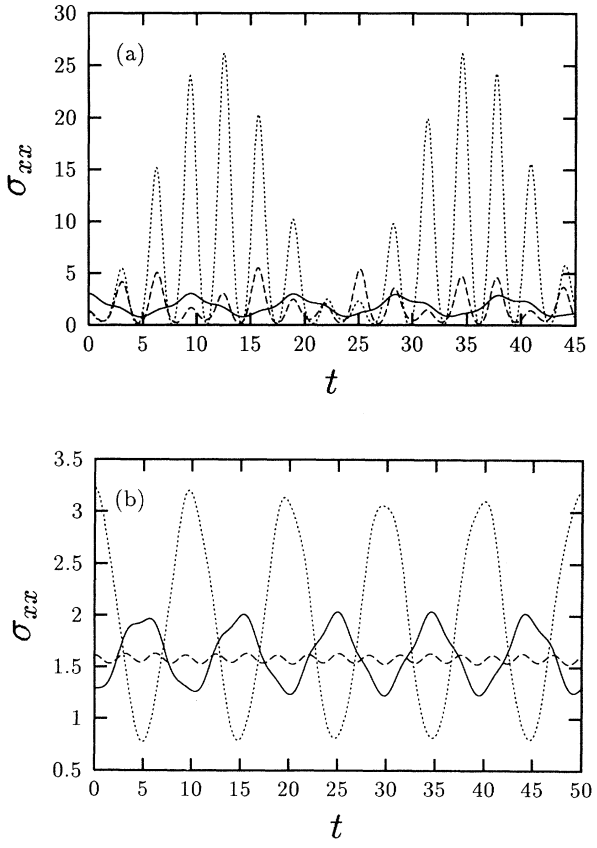

FIG. 2. Variance σ_{xx} vs time t for for various amplitudes of the parametric modulation and different squeezing parameter at $\omega_0^2 = 0.1$. (a) $r = 0.3$. The solid line corresponds to $\epsilon = 0.1$, the dashed line to $\epsilon = 0.7$, and the dotted line to $\epsilon = 0.8$. (b) $\epsilon = 0.025$. The solid line corresponds to $r = 1$, the dashed line to $r = 0.8$, and the dotted line to $r = 0.4$.

A. Density matrix

We next derive the density matrix for the dissipative parametric quantum oscillator. To this aim we eliminate the bath and calculate the exact reduced density operator $\rho_R(x_f, y_f, t)$. We make use of the functional integral method of Feynman and Vernon [10].

We start with the Hamiltonian (26). The influence functional formalism then yields for the reduced density matrix

$$\rho_R(x_f, y_f, t) = \int dx_i \int dy_i\, J(x_f, y_f, t|x_i, y_i, 0) \times\rho_R(x_i, y_i, 0), \tag{28}$$

where J is the evolution operator or propagating function of the reduced density matrix. In the case of a factorizing initial state the reduced initial density matrix $\rho_R(x_i, y_i, 0)$ is nothing else but $\rho_{\rm osc}(x_i, y_i, 0)$. The propagating function J is given by a twofold path integral

$$J(x_f, y_f, t|x_i, y_i, 0) = \int Dx \int Dy\, \exp\left\{\frac{i}{\hbar}(S[x] - S[y])\right\}\mathcal{F}[x, y], \tag{29}$$

where the integration is over all paths $x(s), y(s), t_0 = 0 \le s \le t$ with $x(t_0 = 0) = x_i$, $y(t_0 = 0) = y_i$, $x(t) = x_f$, and $y(t) = y_f$. The action $S[x]$ of the parametric oscillator reads

$$S[x] = \int_0^t ds\,\frac{1}{2}m\{\dot{x}^2 - [\omega_0^2 + \epsilon\cos(\Omega s + \varphi)]x^2\}. \tag{30}$$

The effect of the environment is included in the influence functional $\mathcal{F}$ [18]

$$\mathcal{F}[x,y] = \exp\left\{\frac{i}{\hbar}\frac{m}{2}\left[(x_i+y_i)\int_0^t ds\,\gamma(s)[x(s)-y(s)] + \int_0^t ds\int_0^s du\,\gamma(s-u)[\dot{x}(u)+\dot{y}(u)][x(s)-y(s)]\right]\right\}$$
$$\times \exp\left\{-\frac{1}{\hbar}\int_0^t ds\int_0^s d\tau\,[x(\tau)-y(\tau)]K(\tau-s)[x(s)-y(s)]\right\}. \quad (31)$$

$K(s)$ denotes the noise kernel

$$K(s) = \int_0^\infty \frac{d\omega}{\pi}\coth\left(\frac{\omega\hbar}{2k_BT}\right)\cos(\omega s)I(\omega), \quad (32)$$

wherein k_B denotes the Boltzmann constant and T denotes the temperature of the bath. The friction kernel $\gamma(s)$ reads in terms of spectral density

$$\gamma(s) = \frac{2}{m}\int_0^\infty \frac{d\omega}{\pi}\frac{I(\omega)}{\omega}\cos\omega s.$$

For an Ohmic heat bath these quantities are given by

$$K(s) = m\gamma\int_0^\infty \frac{d\omega}{\pi}\omega\coth\left(\frac{\omega\hbar}{2k_BT}\right)\cos(\omega s),$$
$$\gamma(s) = 2\gamma\delta(s). \quad (33)$$

Since the path integrals in J are quadratic, they can be done exactly to yield

$$J(x_f,y_f,t|x_i,y_i,0)$$
$$= \frac{1}{N(t)}\exp\left\{\frac{i}{\hbar}(S[x_{\rm cl}]-S[y_{\rm cl}])\right\}\mathcal{F}[x_{\rm cl},y_{\rm cl}]. \quad (34)$$

The functions $x_{\rm cl}, y_{\rm cl}$ denote the classical paths and N is a normalization factor. Introducing the sum and difference variables, i.e.,

$$q = x-y, \qquad Q = \frac{1}{2}(x+y), \quad (35)$$

the minimal action paths are given as the solutions to the equations

$$\ddot{q}(s) - \gamma\dot{q}(s) + \omega^2(s;\varphi)q(s) = -2q_f\gamma\delta(t-s), \quad (36)$$

$$\ddot{Q}(s) + \gamma\dot{Q}(s) + \omega^2(s;\varphi)Q(s) = -2Q_i\gamma\delta(s), \quad (37)$$

with the boundary conditions $q(0)=q_i$, $q(t)=q_f$, $Q(0)=Q_i$, $Q(t)=Q_f$, and $\omega^2(s;\varphi)=\omega_0^2+\epsilon\cos(\Omega s+\varphi)$. The inhomogeneities on the right-hand side of (36) and (37) arise because of the first term on the right-hand side of the influence functional in (31). In the work of Caldeira and Leggett [11] these terms were omitted.

In the case of a time-independent harmonic oscillator the solutions of (36) and (37) are connected through $q(s)=Q(t-s)$. With a time-dependent frequency this is no longer true. Hence one has to be careful in using results from the literature for stationary problems [18,19].

Equations (36) and (37) are solved with

$$q(s) = v_1(t,s;\varphi)q_i + v_2(t,s;\varphi)q_f \qquad \text{for } s<t, \quad (38)$$
$$Q(s) = u_1(t,s;\varphi)Q_i + u_2(t,s;\varphi)Q_f$$
$$+2\gamma f_1(s;\varphi)[1-\Theta(s)]Q_i \qquad \text{for all } s, \quad (39)$$

with $\Theta(s)$ denoting the step function $\Theta(s<0)=0$, $\Theta(0)=1/2$, and $\Theta(s>0)=1$. Here we defined solutions to the homogeneous part of Eqs. (36) and (37) that fulfill $u_1(t,0;\varphi)=v_1(t,0;\varphi)=1$, $u_1(t,t;\varphi)=v_1(t,t;\varphi)=0$, $u_2(t,0;\varphi)=v_2(t,0;\varphi)=0$, and $u_2(t,t;\varphi)=v_2(t,t;\varphi)=1$. For u_1 and u_2 we obtain

$$u_1(t,s;\varphi) = f_2(s;\varphi) - f_1(s;\varphi)\frac{f_2(t;\varphi)}{f_1(t;\varphi)},$$
$$u_2(t,s;\varphi) = \frac{f_1(s;\varphi)}{f_1(t;\varphi)}, \quad (40)$$

with $f_i(s;\varphi)=\phi_i(s;\varphi)e^{-\gamma s/2}$, $i=1,2$, and $\phi_i(s;\varphi)$ given in (8). The functions v_1 and v_2 read

$$v_1(t,s;\varphi) = \left[f_2(s;\varphi) - f_1(s;\varphi)\frac{f_2(t;\varphi)}{f_1(t;\varphi)}\right]e^{\gamma s},$$
$$v_2(t,s;\varphi) = \frac{f_1(s;\varphi)}{f_1(t;\varphi)}e^{\gamma(s-t)}. \quad (41)$$

The inhomogeneity in Eq. (37) is reflected by the step-function contribution in (39). But we neglected the inhomogeneity in Eq. (36). We considered the solution of (36) only in the regime $[0,t)$, because during this time there is no influence of the inhomogeneity. The solution is continuous at $s=t$ [and because of the boundary conditions $q(t)=q_f$], but its first derivative jumps at that point. Because we need only the derivative of $Q(s)$, and not of $q(s)$, to calculate the propagating function we can neglect this jump; cf. (36). Inserting these solutions into Eq. (34) leads to the main result

$$J(q_f,Q_f,t|q_i,Q_i,0) = \frac{1}{N(t)}\exp\left[-\frac{1}{\hbar}\{a_{11}(t;\varphi)q_i^2 + [a_{12}(t;\varphi)+a_{21}(t;\varphi)]q_iq_f + a_{22}(t;\varphi)q_f^2\}\right] \quad (42)$$

$$\times\exp\left[-\frac{i}{\hbar}m\{[b_3(t;\varphi)q_i - b_4(t;\varphi)q_f]Q_f + [b_1(t;\varphi)q_i - b_2(t;\varphi)q_f]Q_i\}\right], \quad (43)$$

with

$$a_{ij}(t;\varphi) = \frac{1}{2}\int_0^t ds_1 \int_0^t ds_2\, v_i(t,s_1;\varphi)v_j(t,s_2;\varphi) \times K(s_1 - s_2)$$

and

$$b_1(t;\varphi) = \dot{u}_1(t,0;\varphi) + \gamma, \qquad b_2(t;\varphi) = \dot{u}_1(t,t;\varphi),$$
$$b_3(t;\varphi) = \dot{u}_2(t,0;\varphi), \qquad b_4(t;\varphi) = \dot{u}_2(t,t;\varphi). \quad (44)$$

Here the overdot denotes the derivative with respect to s, i.e., $\dot{u}_1(t,0) = [\partial u_1(t,s)/\partial s]|_{s=0}$. The normalization factor $N(t)$ can be determined from the conservation of normalization of the density matrix

$$\int dQ_f\, \rho_R(Q_f, q_f = 0, t) = \frac{1}{N(t)}\frac{2\pi\hbar}{b_3(t;\varphi)} = 1, \quad (45)$$

where we use

$$\int dQ_f\, Q_f^n \exp\left[\frac{i}{\hbar}b_3(t;\varphi)\, q_i Q_f\right] = -\frac{2\pi\hbar}{b_3(t;\varphi)}\left(\frac{\hbar}{ib_3(t;\varphi)}\frac{\partial}{\partial q_i}\right)^n \delta(q_i). \quad (46)$$

This yields for $N(t)$

$$N(t) = \frac{2\pi\hbar}{b_3(t;\varphi)}. \quad (47)$$

Equation (28) together with (43) and (47) gives the exact reduced density matrix for times t when $f_1(t;\varphi) \neq 0$.

B. Master equation and Wigner transformation

We investigate here the equation of motion for the reduced density operator. By use of the Wigner distribution function we compare this equation with the equation for a classical Brownian particle, the Fokker-Planck equation. This provides a possibility to discuss the connection with the classical system.

To derive the master equation from the propagating function of the reduced density matrix we take first the time derivative of both sides of Eq. (43). Then we multiply both sides by $\rho_R(q_i, Q_i, 0)$ and integrate over Q_i and q_i. In this way one arrives at the central result

$$i\hbar\frac{\partial}{\partial t}\rho_R(x,y,t) = \left[-\frac{\hbar^2}{2m}\left(\frac{\partial^2}{\partial x^2} - \frac{\partial^2}{\partial y^2}\right) + \frac{m}{2}\omega^2(t;\varphi)(x^2 - y^2)\right]\rho_R(x,y,t)$$
$$- \frac{i\hbar\gamma}{2}(x-y)\left(\frac{\partial}{\partial x} - \frac{\partial}{\partial y}\right)\rho_R(x,y,t) + iD_{pp}(t,0)(x-y)^2\rho_R(x,y,t)$$
$$- \frac{\hbar}{m}[D_{xp}(t,0) + D_{px}(t,0)](x-y)\left(\frac{\partial}{\partial x} + \frac{\partial}{\partial y}\right)\rho_R(x,y,t), \quad (48)$$

where D_{pp}, D_{px}, and D_{xp} are given by [see Eq. (44)]

$$D_{pp}(t,0) = 2\left(b_4 + \frac{\dot{b}_2}{b_2}\right)a_{22} - \dot{a}_{22} + 2\frac{\dot{b}_2 b_4}{b_2 b_3}a_{12} - 2\frac{b_4}{b_3}\dot{a}_{12},$$
$$D_{px}(t,0) = D_{xp}(t,0) = -\frac{1}{b_3}\dot{a}_{12} + a_{22} + \frac{\dot{b}_2}{b_3 b_2}a_{12}. \quad (49)$$

The first term in the large square brackets on the right-hand side of the *exact equation* (48) corresponds to the Liouvillian evolution. The second term proportional to γ is a dissipative term and all the remaining terms are diffusive terms with *time-dependent* coefficients. In contrast to the classical limit (see below) the master equation involves a cross diffusion $D_{px}(t,0) = D_{xp}(t,0)$.

Although the system unter consideration is time dependent the diffusive term D_{xx} equals zero like in the case of the harmonic oscillator. The term D_{xx} has the form $D_{xx}(t,0) = (2a_{12} - \dot{a}_{11}/b_3)/b_3$. Because of the identity $\dot{a}_{11} = -2\dot{v}_1(t)a_{12}$ it is necessary that

$$\dot{v}_1(t,t;\varphi) = -\dot{u}_2(t,0;\varphi) \quad (50)$$

to make D_{xx} disappear. This relation is valid for an undriven harmonic oscillator because $v_1(t,s;\varphi) = u_2(t,t-s;\varphi)$. In addition, the condition (50) is also valid for a parametric oscillator, due to the time independence of the Wronskian (9):

$$\dot{v}_1(t,t;\varphi) = \frac{\dot{f}_2(t;\varphi)f_1(t;\varphi) - f_2(t;\varphi)\dot{f}_1(t;\varphi)}{f_1(t;\varphi)}e^{\gamma t}$$
$$= \frac{\dot{\phi}_2(t;\varphi)\phi_1(t;\varphi) - \phi_2(t;\varphi)\dot{\phi}_1(t;\varphi)}{f_1(t;\varphi)}$$
$$= -\frac{1}{f_1(t;\varphi)} = -\dot{u}_2(t,0;\varphi).$$

To gain insight into the phase-space structure of the driven dynamics we consider the Wigner transform of ρ_R, which is defined by

$$F_W(Q,p,t) = \frac{1}{2\pi\hbar}\int_{-\infty}^{\infty} dq\, \rho_R\left(Q - \frac{q}{2}, Q + \frac{q}{2}, t\right)e^{ipq/\hbar}. \quad (51)$$

With (51) we find by virtue of Eq. (48) that $F_W(Q,p,t)$ obeys the Fokker-Planck-like equation

$$\frac{\partial}{\partial t}F_W(Q,p,t)$$

$$= \left\{ -\frac{1}{m}p\frac{\partial}{\partial Q} + m\omega^2(t;\varphi)Q\frac{\partial}{\partial p} + \gamma\frac{\partial}{\partial p}p \right.$$
$$\left. -\hbar D_{pp}(t,0)\frac{\partial^2}{\partial p^2} - \frac{\hbar}{m}[D_{xp}(t,0)+D_{px}(t,0)]\frac{\partial^2}{\partial Q\partial p} \right\}$$
$$\times F_W(Q,p,t). \tag{52}$$

For high temperatures ($T \to \infty$) we can calculate the diffusion coefficients D_{pp} and D_{xp} explicitly because $K(s)$ takes on the form

$$K(s) = \frac{2\gamma D}{\hbar}\delta(s), \qquad D = k_B T. \tag{53}$$

They are given as

$$D_{xp} = 0, \quad D_{pp} = -\frac{\gamma D}{\hbar}. \tag{54}$$

Therefore, Eq. (52) for $T \to \infty$ takes on the form of the classical Fokker–Planck equation that is discussed in detail in Ref. [20],

$$\frac{\partial}{\partial t}F_W(Q,p,t) = \left\{ -\frac{1}{m}p\frac{\partial}{\partial Q} + m\omega^2(t;\varphi)Q\frac{\partial}{\partial p} \right.$$
$$\left. +\gamma\frac{\partial}{\partial p}p + \gamma D\frac{\partial^2}{\partial p^2} \right\} F_W(Q,p,t). \tag{55}$$

C. Mean values and variances

The expectation value $\langle f(x)\rangle$ of a variable f, being a function of the coordinate x alone, is given by

$$\langle f(x)\rangle = \int dQ_f\, f(Q_f)\rho_R(Q_f, q_f = 0, t)$$
$$= \int dQ_f \int dQ_i \int dq_i\, f(Q_f)$$
$$\times J(Q_f, q_f = 0, t|Q_i, q_i, 0)\rho_R(Q_i, q_i, 0). \tag{56}$$

The first moments read in terms of the initial values $\langle x(t_0 = 0;\varphi)\rangle = \langle x_0\rangle$ and $\langle p(t_0 = 0;\varphi)\rangle = \langle p_0\rangle$

$$\langle x(t;\varphi)\rangle = [f_2(t;\varphi) - \frac{\gamma}{2}f_1(t;\varphi)]\langle x_0\rangle + \frac{1}{m}f_1(t;\varphi)\langle p_0\rangle, \tag{57}$$

$$\langle p(t;\varphi)\rangle = m\frac{d}{dt}\langle x(t;\varphi)\rangle$$
$$= m[\dot f_2(t;\varphi) - \frac{\gamma}{2}\dot f_1(t;\varphi)]\langle x_0\rangle + \dot f_1(t;\varphi)\langle p_0\rangle. \tag{58}$$

The evolution of $\langle p(t;\varphi)\rangle$ is discontinuous at $t_0 = 0$, i.e., $\lim_{t\to 0+}\langle p(t;\varphi)\rangle = \langle p_0\rangle - m\gamma\langle x_0\rangle/2$ is in general not equal to $\langle p_0\rangle$. This instantaneous jump of $\langle p(t;\varphi)\rangle$ can be removed with an environmental cutoff ω_c, or a nonfactorizing initial state [18].

The variances are obtained accordingly. They are given by

$$\sigma_{xx}(t;\varphi) = \left(f_2 - \frac{\gamma}{2}f_1\right)^2\sigma^0_{xx} + \frac{2}{m}f_1\left(f_2 - \frac{\gamma}{2}f_1\right)\sigma^0_{xp}$$
$$+\frac{1}{m^2}f_1^2\sigma^0_{pp} + \frac{2\hbar}{m}f_1^2 a_{11}, \tag{59}$$

$$\sigma_{xp}(t;\varphi) = m\left[f_2\dot f_2 - \frac{\gamma}{2}\left(f_1\dot f_2 + \dot f_1 f_2 - \frac{1}{2}\gamma f_1\dot f_1\right)\right]\sigma^0_{xx}$$
$$+\frac{1}{2}(f_1\dot f_2 + \dot f_1 f_2 - \gamma f_1\dot f_1)\sigma^0_{xp}$$
$$+ f_1\dot f_1\sigma^0_{pp} + 2\hbar(f_1\dot f_1 a_{11} + f_1 a_{12}), \tag{60}$$

$$\sigma_{pp}(t;\varphi) = m^2\left(\dot f_2 - \frac{\gamma}{2}\dot f_1\right)^2\sigma^0_{xx} + 2m\dot f_1\left(\dot f_2 - \frac{\gamma}{2}\dot f_1\right)\sigma^0_{xp}$$
$$+\dot f_1^2\sigma^0_{pp} + 2\hbar m(2\dot f_1^2 a_{11} + \dot f_1 a_{12} + a_{22}). \tag{61}$$

where we omitted the arguments of the functions $a_{ij}(t;\varphi)$, and $f_i(t;\varphi)$ for better lucidity. We also used that $a_{12}(t;\varphi) = a_{21}(t;\varphi)$ and termed the initial variances at $t_0 = 0$ as σ^0_{xx}, σ^0_{xp}, and σ^0_{pp}, respectively. The expressions containing the initial values describe the transient behavior and are damped out in the course of time; the remaining terms contain the long time behavior.

D. Numerical results

To get explicit results we calculate the variances numerically. For that purpose we insert the functions $\phi_1(t;\varphi)$ and $\phi_2(t;\varphi)$, which we determined via a numerical integration of the differential equation (2) into Eqs. (59)–(61). The Ohmic damping leads to a divergence in σ_{pp}, just as in the case of a damped harmonic oscillator [18,21]. We introduce a sharp high-frequency cutoff ω_c of the bath frequencies ω in the frequency integral of $K(t)$ (33) to remove this divergence. This is correct as long as we consider only times that are large compared to ω_c^{-1}. A more appealing procedure would be to regularize the divergent quantities with a high-frequency cutoff in the spectral density of the heat bath.

The results are plotted in Fig. 3. Figure 3(a) shows $m\Omega\sigma_{xx}(t;\varphi)/2\hbar$ for increasing modulation amplitude ϵ. The initial values of the variances are analogous to that in Sec. III, i.e., $\sigma^0_{xx} = \hbar/2mr\sqrt{\omega_0^2+\epsilon}$, $\sigma^0_{xp} = 0$, and $\sigma^0_{pp} = \hbar r m\sqrt{\omega_0^2+\epsilon}/2$. The ϵ values $\epsilon = 0, 0.5, 1$ lead to decaying solutions of the damped Mathieu equation, i.e., $\langle x(t;\varphi)\rangle \to 0$ as $t \to \infty$. After a short time, $\sigma_{xx}(t;\varphi)$ becomes a constant for $\epsilon = 0$ (dissipative harmonic oscillator), whereas for the other two values of ϵ it becomes a *periodic function* that oscillates with the frequency Ω. This frequency is *not affected* by the strength of the friction γ. The amplitude of the oscillations increases with increasing modulation strenghth ϵ. For ϵ in the unstable region, the variances, as well as any other moment, become unbounded, as can be seen for $\epsilon = 2$. In Fig. 3(b) we start with a squeezed state and compare it with the

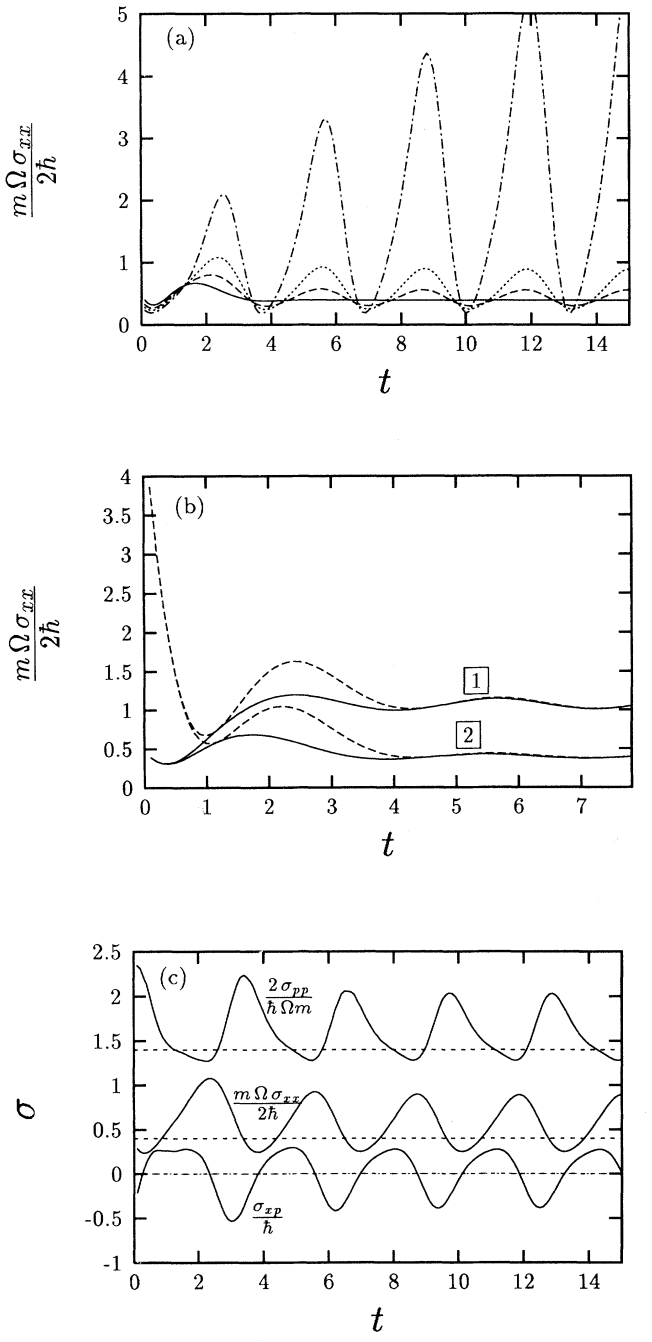

FIG. 3. (a) Scaled position variance $m\Omega\sigma_{xx}/2\hbar$ vs time t at $\omega_0^2 = 1$, $\gamma = 1$, $\Omega = 2$, $\omega_c = 50$, $\varphi = 0$, $k_BT/\hbar\omega_0 = 0.1$, and $r = 1$ for different values of the parametric modulation ϵ. The solid line corresponds to $\epsilon = 0$, the dashed line to $\epsilon = 0.5$, the dotted line to $\epsilon = 1$, and the dot-dashed line to $\epsilon = 2$. (b) Scaled position variance $m\Omega\sigma_{xx}/2\hbar$ vs time t at $\omega_0^2 = 1$, $\gamma = 1$, $\Omega = 2$, $\omega_c = 50$, $\varphi = 0$, and $\epsilon = 0.1$ for varying squeezing parameters and different initial temperatures of the bath. The dashed lines correspond to $r = 0.1$ and the solid lines to $r = 1$. For the lines marked with 2, $k_BT/\hbar\omega_0 = 0.1$; for 1, $k_BT/\hbar\omega_0 = 1$. (c) Plot of all three variances $m\Omega\sigma_{xx}/2\hbar$, $\sigma_{xp}/\hbar$, and $2\sigma_{pp}/\hbar\Omega m$ as a function of time t at $\omega_0^2 = 1$, $\gamma = 1$, $\Omega = 2$, $\omega_c = 50$, $\varphi = 0$, $k_BT/\hbar\omega_0 = 0.1$, and $\epsilon = 1$. The dashed lines correspond to the equilibrium values at $\epsilon = 0$.

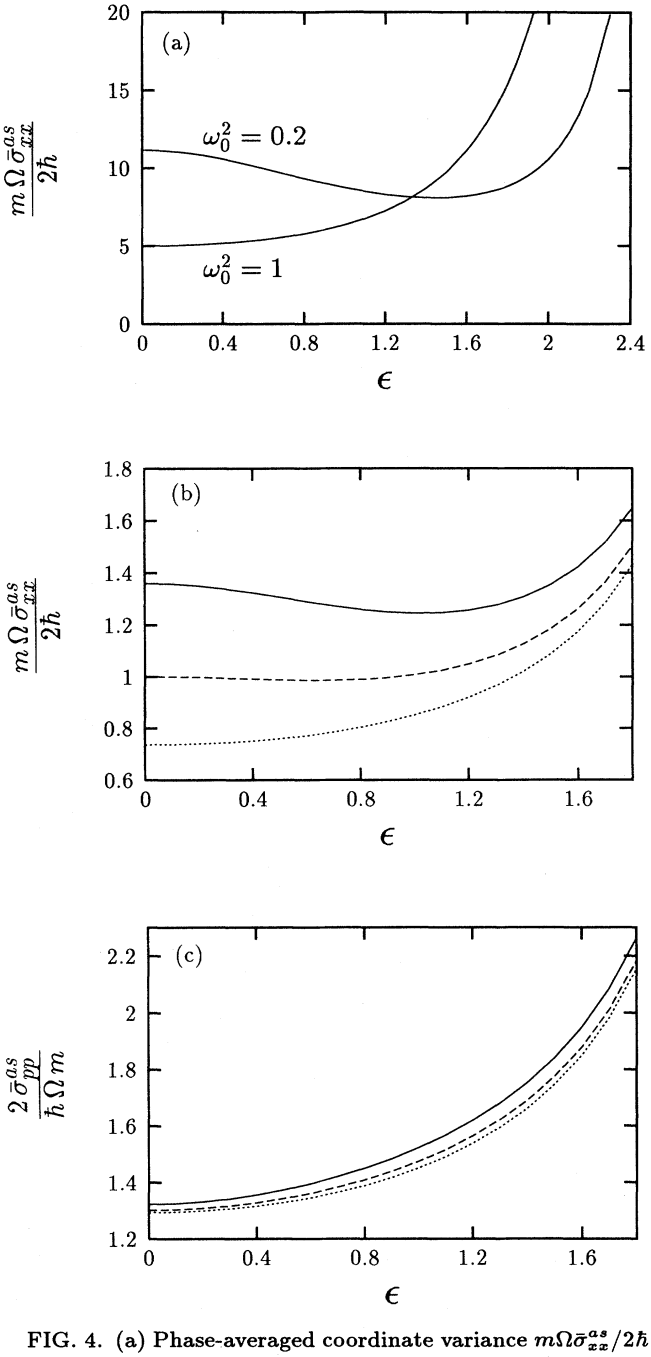

FIG. 4. (a) Phase-averaged coordinate variance $m\Omega\bar{\sigma}_{xx}^{as}/2\hbar$ as a function of the modulation ϵ at $\gamma = 1$, $k_BT/\hbar\omega_0 = 5$, $\omega_c = 50$, and $\Omega = 2$ for two different values of the angular frequency $\omega_0^2 = 0.2$ and $\omega_0^2 = 1$. (b) Phase-averaged coordinate variance $m\Omega\bar{\sigma}_{xx}^{as}/2\hbar$ as a function of the modulation ϵ at $\gamma = 1$, $\omega_0^2 = 0.2$, $\omega_c = 50$, and $\Omega = 2$ for different values of the initial heat bath. The solid line corresponds to $k_BT/\hbar\omega_0 = 0.5$, the dashed line corresponds to $k_BT/\hbar\omega_0 = 0.3$, and the dotted line corresponds to $k_BT/\hbar\omega_0 = 0.1$. (c) Phase-averaged momentum variance $2\sigma_{pp}^{as}/\hbar\Omega m$ as a function of the modulation ϵ at $\gamma = 1$, $\omega_0^2 = 0.2$, $\omega_c = 50$, and $\Omega = 2$ for different values of the initial heat bath. The solid line corresponds to $k_BT/\hbar\omega_0 = 0.5$, the dashed line corresponds to $k_BT/\hbar\omega_0 = 0.3$, and the dotted line corresponds to $k_BT/\hbar\omega_0 = 0.1$.

nonsqueezed state. As an interesting result we find that the effect of initial squeezing relaxes on a fast time scale. This relaxation time depends only weakly on temperature, but depends on the strength of the Ohmic friction γ. This feature is in accordance with results for the relaxation of an initially squeezed state for the damped quantum oscillator [18]. For reasons of comparison we depict $\sigma_{xx}(t;\varphi)$, $\sigma_{xp}(t;\varphi)$, $\sigma_{pp}(t;\varphi)$, and the equilibrium ($\epsilon = 0$) values in Fig. 3(c).

The minima of the time-periodic variances are smaller than the respective equilibrium values, which are indicated by dashed lines. Hence, with a stroboscopic measurement, which only probes these minima, this behavior can be used to *reduce the fluctuations in either the momentum or coordinate variable.* This feature likely can be of use in applications that aim at reducing (or enhancing) the fluctuational properties, such as, e.g., for effectively lowering the temperature (i.e., σ_{pp}) or diminishing the spatial width of particle fluctuations.

These calculations of the variances required the knowledge of the initial phase φ of the modulation. Since in an experimental situation, in general, the phase is not known, we next *average* over the uniformly distributed phase φ. For $t \to \infty$ this procedure becomes equivalent to an average over time. The asymptotic (i.e., $t \to \infty$) time-independent phase-averaged values of σ_{xx} and σ_{pp}, i.e., $\bar{\sigma}^{as}_{xx}$ and $\bar{\sigma}^{as}_{pp}$, are depicted in Fig. 4. We consider only parameter values that lie within the stable regions of the parameter space. The behavior of $\bar{\sigma}^{as}_{xp}$ is not depicted because it equals zero for all parameter values. It can be noted from Fig. 4(a) that for positive-valued ω_0^2, being smaller than some threshold value $\omega_0^2 \approx 0.5$, $\bar{\sigma}^{as}_{xx}$ first decreases with increasing ϵ, goes through a minimum, and then increases again. Above this threshold value, $\bar{\sigma}^{as}_{xx}$ increases monotonically. This typical feature is distinct from the behavior of a driven harmonic oscillator. Decreasing the temperature not only reduces $\bar{\sigma}^{as}_{xx}$, but also changes the form of the function: The minimum disappears with decreasing temperatures of the heat bath, an effect that can clearly be detected from Fig. 4(b). In clear contrast to the behavior of the position variance, the corresponding phase-averaged momentum variance always monotonically increases with increasing ϵ; cf. Fig. 4(c).

V. CONCLUSIONS

In summary, we have studied the mean values and the temperature-dependent variances for dissipative parametric quantum Brownian motion. For Ohmic friction we give the explicit result for the reduced density matrix in Sec. IV A. The rate of change of this density matrix, or its corresponding Wigner representation in phase space, obeys an exact Fokker-Planck-like equation with time-dependent drift and diffusion coefficients that depend on the Mathieu solutions for the damped parametric oscillator. The stable variances undergo asymptotic periodic oscillations with the minima lying below the corresponding equilibrium values for σ_{xx}, σ_{pp}, and σ_{xp}, respectively; cf. Fig. 3(c). This interesting feature may be of use for applications that are tailored to reduce the influence of noise on trapped particles.

In presence of Ohmic friction, the effect of initial squeezing of variances decays on a rather rapid time scale; cf. Fig. 3(b). The time-averaged position variance exhibits a minimum for sufficiently high temperatures and sufficiently small ω_0^2. In contrast, the averaged momentum variance is monotonically increasing with strength ϵ of the parametric modulation.

[1] F. Grossmann, T. Dittrich, P. Jung, and P. Hänggi, Phys. Rev. Lett. **67**, 516 (1991); F. Grossmann and P. Hänggi, Europhys. Lett. **18**, 571 (1992); I. Plata and J. M. Gomez-Llorente, Phys. Rev. A **48**, 782 (1993); R. Bavli and H. Metiu, *ibid.* **47**, 3299 (1993); R. I. Lukier and M. Morillo, Chem. Phys. **183**, 375 (1994); T. Dittrich, B. Oelschlägel, and P. Hänggi, Europhys. Lett. **22**, 5 (1993); M. Grifoni, M. Sassetti, J. Stockburger, and U. Weiss, Phys. Rev. E **48**, 3497 (1993); M. Wagner, Phys. Rev. A **51**, 798 (1995).

[2] P. Hänggi and C. Zerbe, in *Noise in Physical Systems and 1/f Fluctuations*, edited by P. H. Handel and A. L. Chung, AIP Conf. Proc. No. 285 (AIP, New York, 1993), p. 481.

[3] L. S. Brown, Phys. Rev. Lett. **66**, 527 (1991).

[4] M. Combescure, Ann. Inst. Henri Poincaré A **44**, 293 (1986).

[5] C. F. Lo, J. Phys. A **23**, 1155 (1990).

[6] L. S. Brown, Phys. Rev. A **36**, 2463 (1987).

[7] R. J. Rubin, Phys. Rev. **131**, 964 (1963); G. W. Ford, M. Kac, and P. Mazur, J. Math. Phys. **6**, 504 (1965); P. Ullersma, Physica (Utrecht) **32**, 27 (1966); **32**, 56 (1966); **32**, 74 (1966); **32**, 90 (1966).

[8] R. Zwanzig, J. Stat. Phys. **9**, 215 (1973).

[9] A. J. Leggett, S. Chakravarty, A. T. Dorsey, M. P. A. Fisher, A. Garg, and W. Zwerger, Rev. Mod. Phys. **59**, 1 (1987); H. Grabert, P. Schramm, G.-L. Ingold, Phys. Rep. **168**, 115 (1988); P. Hänggi, P. Talkner, and M. Borkovec, Rev. Mod. Phys. **62**, 251 (1990), Sec. IV; U. Weiss, *Quantum Dissipative Systems* (World Scientific, Singapore, 1993); V. A. Benderskii, D. A. Makarov, and Ch. A. Wright, Adv. Chem. Phys. **88** (1994).

[10] R. P. Feynman and F. L. Vernon, Ann. Phys. (N.Y.) **24**, 118 (1963).

[11] A. O. Caldeira and A. J. Leggett, Physica A **121**, 587 (1983); **130**, 374 (1985).

[12] N. W. McLachlan, *Theory and Application of Mathieu Functions* (Dover, New York, 1964); A. H. Nayfeh and D. T. Mook, *Nonlinear Oscillations* (Wiley, New York, 1979).

[13] J. H. Shirley, Phys. Rev. **138**, B979 (1965); Ya. B. Zel'dovich, Zh. Eksp. Teor. Fiz. **51**, 1492 (1966) [Sov. Phys. JETP **24**, 1006 (1967)]; V. I. Ritus, *ibid.*

51, 1544 (1966) [*ibid.* **24**, 1041 (1967)].
[14] A. M. Perelomov and V. S. Popov, Teor. Mat. Fiz. **1**, 360 (1969).
[15] K. Husimi, Prog. Theor. Phys. **9**, 381 (1953).
[16] J. Rezende, J. Math. Phys. **25**, 3264 (1984).
[17] A. O. Caldeira and A. J. Leggett, Ann. Phys. (N.Y.) **149**, 374 (1983); **153**, 445 (1984).
[18] H. Grabert, P. Schramm, and G.-L. Ingold, Phys. Rep. **168**, 115 (1988).
[19] B. L. Hu, J. P. Paz, and Y. Zhang, Phys. Rev. D **45**, 2843 (1992).
[20] C. Zerbe, P. Jung, and P. Hänggi, Phys. Rev. E **49**, 3626 (1994).
[21] P. Riseborough, P. Hänggi, and U. Weiss, Phys. Rev. A **31**, 471 (1985).